Malaysian Journal of Chemistry, 2024, Vol. 26(5), 90-100
(Special Issue: *3rd Virtual International Symposium on Sciences 2023*)

Modification of Screen-Printed Carbon Electrode with Nanogold for Detection of Glucose

Nur Zulaikha Fakhruddin[1], Yusairie Mohd[2] and Mohammad Hafizudden Mohd Zaki[3]*
[1]Faculty of Applied Sciences, Universiti Teknologi MARA (UiTM) Shah Alam, 40450 Shah Alam, Selangor, Malaysia
[2]Electrochemical Materials and Sensor (EMaS) Research Group, Universiti Teknologi MARA (UiTM) Shah Alam, 40450 Shah Alam, Selangor, Malaysia
[3]Department of Chemistry, Faculty of Applied Sciences, Universiti Teknologi MARA, Jengka, Pahang, Malaysia
*Corresponding author (e-mail: hafizudden@uitm.edu.my)

The properties of screen-printed carbon electrodes (SPCE) with nanogold (AuNP) were ascertained to detect glucose samples. The electrodes were modified with different potentials to obtain suitable potentials for the detection of glucose. The potentials used to prepare gold electrodes were -0.8 V, +0.56 V, and +0.9 V. The bare SPCE acted as a comparison between the bare and the modified SPCE. The modified electrodes (AuNP/SPCE) were characterised using Field Emission Scanning Electron Microscopy (FESEM), Energy Dispersive X-ray (EDX), and X-ray Diffraction (XRD) with deposition at -0.8 V and +0.56 V, proving that the gold nanostructures were deposited at the SPCE surface. The deposition at +0.9 V had an insignificant amount of Au on the SPCE surface, similar to bare SPCE. The active sites and reversibility of the gold electrode can be determined by measuring the electrochemical active surface area (ECSA) of electrode and its anodic and cathodic peak current density ratio (Ipa/Ipc), respectively. The ECSA for modified SPCE with different potentials of -0.8 V, +0.56 V, and +0.9 V were 6.873 cm^2, 0.786 cm^2, and 0.253 cm^2, respectively. The Ipa/Ipc ratio of +0.56 V and -0.8 V showed excellent reversibility and transfer rate compared to +0.9 V. Thus, deposition at -0.8 V and +0.56 V was chosen to detect glucose, and the sensitivity and limit of detection (LOD) were calculated. The sensitivity and LOD for these two modified electrodes (-0.8 V and +0.56 V) were 7.53 $mA.mM^{-1}cm^{-2}$ and 14.73 mM, as well as 73.38 $mA.mM^{-1}cm^{-2}$ and 13.13 mM, respectively.

Keywords: Different potentials; glucose; nanogold electrode; screen-printed carbon electrode

Received: November 2023; Accepted: February 2024

Glucose, also known as monosaccharide sugar, is a carbohydrate that can be found in the human body. Glucose supplies energy to all of the cells in the body except for cardiac myocytes. The excessive glucose will be stored in the liver in the form of glycogen. However, with food consumption that is unhealthy and sugary, the glucose cannot be stored in the liver and keeps flowing in the blood. The World Health Organization (WHO) stated that there are currently 422 million people suffering from diabetes mellitus worldwide, and there are around 1.5 million individuals who die from diabetes each year [1]. In order to regulate diabetes, as well as in food processing, biotechnology, and environmental protection, it is essential to assess our body's glucose level. Thus, it is important to develop a highly sensitive, simple, and cost-effective method to determine the glucose level in the current lifestyle. The determination of glucose has been studied using a variety of techniques, including luminescence, colorimetry, fluorescence-based analysis, flow injection analysis, as well as optical and electrochemical transductions [2].

Electrochemical sensing is one of the most promising and widely used techniques for the detection of glucose in the current environment because of its quick reaction, convenience of use, dependability, good sensitivity, low cost, and portability. Modern methods like screen printing are used to create sensitive and portable electrochemical sensors that are small and light. It has been used in practically all fields of chemistry, including clinical tests, environmental analysis, and food processing [3]. Although screen-printed carbon electrode (SPCE) is one of the most used materials because it is versatile and cheap, the heterogeneous kinetics of working electrodes on SPCE surfaces are slow and require electrochemical activation of inks such as platinum, gold, or silver materials to improve electron transfer rates [4]. The recent rapid development of nanotechnology has expanded the manufacturing and utilisation of nanoparticles. Nanoporous gold has expanded greatly in these years because of its intriguing material properties, such as its high specific surface area, easy surface modification prospects, high selectivity, electrochemical activity, enhanced electrical conductivity, and chemical

†Paper presented at the 3rd Virtual International Symposium on Sciences (3rd VISoS 2023)

stability [5]. A research study by Francis & Knospe concluded that interfacial impedances derive from the effective area of nanoporous gold electrodes to planar gold electrodes are very low (>40×) compared to other conventional electrodes [6]. Furthermore, Liu and co-workers stated that AuNPs are particularly suitable for electrochemical sensing due to their biocompatibility, high binding affinity to thiol-containing molecules, and good conductivity [7]. The nanoporous material can increase the electrode's surface area and the number of immobilised DNA probes.

Nanogold or nanoporous gold can be synthesised using a fabrication technique, as reported by Sondhi & Stine [5]. There are four fabrication techniques stated in the study, which are dealloying, self-assembly, sputter deposition, and electrodeposition. The dealloying method was used for fabricating nanoporous structures with a continuous network of interconnected ligaments and pores of gold [8]. The alloys were fabricated through arc heating, which produced a uniform distribution composition due to equilibrium solidification. This led to the narrow size distribution of nanoporous after dealloying. The self-assembly of the AuNP using aggregation and coalescence produced a porous structure directly, without relying on external assistance [5]. Furthermore, self-assembly monolayers provide a more simple, reproducible, and reliable procedure to immobilise the molecules on various metal surfaces [9]. As for sputter deposition, it is an ideal method to prepare nanometer-thick films with precise control. This deposition control over deposition rate, large area uniformity, high adhesive films, uniform temperature, and the ability to coat diverse substrates. Electro-deposition is usually used in the electroanalytical and catalytic fields to control the morphology of particles, size, and density. Based on Faraday's laws of electrolysis, the mass of gold on the electrode is controlled by the electric charge passed during the electrodeposition process [5].

In this study, the gold nanostructures were deposited on the substrate of a screen-printed electrode by the electrodeposition method at various deposition potentials. The gold coatings formed, known as (AuNP/SPCE) were systematically characterised by various spectroscopy techniques such as Field Emission Scanning Electron Microscope (FESEM), X-ray Diffractometer (XRD), and electrochemical techniques. The electroanalytical performance of the AuNP/SPCE as a sensing electrode was investigated for quantitative detection of glucose by cyclic voltammetry analysis in order to study the sensitivity and selectivity of the prepared gold electrode.

EXPERIMENTAL

Chemicals and Materials

Tetrachloroauric (III) acid trihydrate ($HAuCl_4.3H_2O$), potassium chloride (KCl), sulphuric acid (H_2SO_4), potassium ferrocyanide ($K_4[Fe(CN)_6]$), sodium hydroxide (NaOH), and glucose were used in this study. The screen-printed carbon electrode (SPCE) with a working electrode area of 0.11 cm^2, procured from Metrohm Sdn Bhd, was used in this experiment. The solutions produced were prepared and diluted with deionised water for each procedure. All chemicals were of analytical grade and used as received.

Modification of SPCE with Nanogold

The SPCE surface was directly electrodeposited with nanogold structures using a potentiostatic technique. 10 mM tetrachloroauric (III) acid ($HAuCl_4$) was dissolved in 1.0 M sulphuric acid (H_2SO_4) to create an electrolyte solution for the deposition [10]. A three-electrode electrochemical cell was used in this study, with SPCE serving as the working electrode, a clean platinum serving as the auxiliary electrode, and an electrode made of silver and silver chloride (Ag/AgCl) serving as the reference electrode. An Autolab potentiostat connected to a computer running DropView 8400 software was used in this study. Initially, cyclic voltammetry (CV) was performed by running 10 cycle potential scans between -0.6 V and +1.9 V with a scan rate of 0.1 V/s for the cleaning process of SPCE in a 0.5 M sulphuric acid (H_2SO_4) solution. Then, in order to identify the ideal potential range for the deposition of gold, a single potential scan between -1.0 V and +1.5 V was performed using a 0.1 V/s scan rate in the CV procedure. Following that, chronoamperometry (CA) was used to investigate how different potentials affected the development of gold coatings on the SPCE surface. The deposition potentials selected from the cyclic voltammogram at the reduction potential were +0.9 V, +0.56 V, and -0.8 V. The experiment was conducted at room temperature with a constant deposition time of 1800 seconds [14].

Characterisation and Electrochemical Performance of Coated Nanogold Modified SPCE

The Energy Dispersive X-Ray spectroscopy (EDX) attached to Field Emission Scanning Electron Microscopy (FESEM, Carl Zeiss SMT Supra 40VP) was used to analyse the elemental composition and surface morphology of the produced nanogold structures on SPCE, respectively. X-ray diffraction (XRD, X'pert pro-MPD, PANalytical) was used to determine the crystallographic structure and phase composition of nanogold structures. The electrochemical active surface area (ECSA) of the modified SPCE was calculated from the reduction area of the nanogold structure coating by performing cyclic voltammetry (CV) analysis in a 0.5 M sulphuric acid (H_2SO_4) solution. The reversibility and ability of the electron transfer in the reaction with nanogold electrodes were tested by CV in different concentrations of $K_4[Fe(CN_6)]$, and a 0.1 M KCl solution acted as the supporting electrolyte.

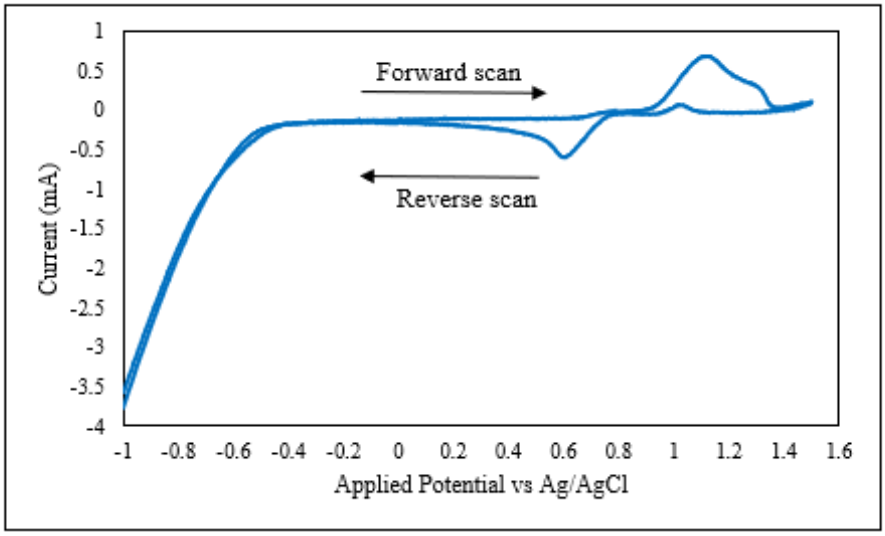

Figure 1. Cyclic voltammogram of SPCE in 10 mM $HAuCl_4$ + 1.0 M H_2SO_4 at 25 °C with a scan rate of 0.1 V/s.

Detection of Glucose by Cyclic Voltammetry Analysis

The glucose sample was dissolved in a 0.1 M sodium hydroxide (NaOH) solution at various concentrations, including 1 mM, 3 mM, 5 mM, 7 mM, and 10 mM concentrations. CV was carried out in a potential range between -0.4 V and +0.8 V at a scan rate of 0.1 V/s and was performed to determine the sensitivity and limit of detection (LOD) of each electrode.

RESULTS AND DISCUSSION

Electrodeposition of Gold on SPCE

Initially, CV was conducted to evaluate the deposition and dissolution processes of gold on the SPCE surface. As indicated in Figure 1, the CV analysis was carried out in a solution of 1.0 M H_2SO_4 and 10 mM tetrachloroauric (III) acid trihydrate ($HAuCl_4$) with a scanning potential of -1.0 V to +1.5 V and switching back to -1.0 V at a scan rate of 0.1 V/s. The reduction of gold was visible in the reverse scan, which caused gold particles to accumulate on the surface of the SPCE. While the oxidation of gold was visible on the forward scan, the Au^{3+} ion in the solution gained three electrons and produced Au particles in the reduction peak, as shown in Reaction 1.

$$Au^{3+}{}_{(aq)} + 3e^- \rightarrow Au_{(s)} \quad (1)$$

The current increased significantly at more negative potentials of -0.4 V to -1.0 V, and this was attributed to hydrogen gas (H_2) evolution, as well as the reduction of gold on the SPCE surface. As seen in Reaction 2, a crossover at -0.4 V on the forward scan indicates the beginning of the hydrogen evolution reaction (HER), which reduced hydrogen ions to hydrogen gas [10].

$$2H^+{}_{(aq)} + 2e^- \rightarrow H_{2\,(g)} \quad (2)$$

From the CV, three reduction potentials were identified and used for the deposition of gold nanostructures on SPCE using Chronoamperometry (CA). The applied potentials chosen were -0.8 V, +0.56 V, and +0.9 V, and deposition time was 1800 s constant for all deposition potentials. Figure 2 shows the chronoamperometric curves for the deposition of gold on SPCE at three different potentials for 1800 s.

The current measured was incredibly low at -0.000018 mA at the deposition potential of +0.9 V and remained constant for 1800 s, indicating negligible charge transfer for the formation of gold on the SPCE surface. At a deposition potential of +0.56 V, the current in the chronoamperometric curve was uniform at -0.088 mA until 1800 s. This suggests that gold on the SPCE surface nucleated uniformly and grew from there. As for the potential range of +0.9 V to +0.56 V, no bubbles were formed on the SPCE surface, indicating that there had been no interference from the evolution of hydrogen gas.

However, the current increased negatively as the deposition time rose when the deposition potential was at -0.8 V. This is because gold was being deposited at the electrode surface at the same time as a substantial HER side reaction [10-11]. The -0.8 V potential showed an unstable current between 200 s and 1800 s, suggesting that a lot of hydrogen bubbles were vigorously formed on the electrode surface.

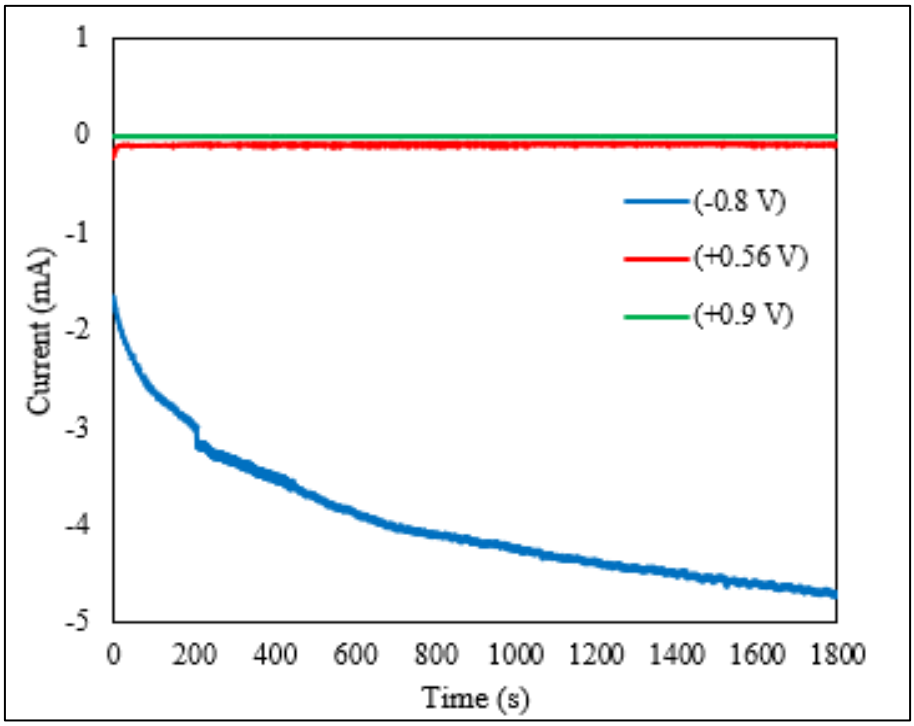

Figure 2. Chronoamperometric curves of gold electrodeposition onto SPCE with applying different potentials of -0.8 V, +0.56 V, and +0.9 V for 1800s.

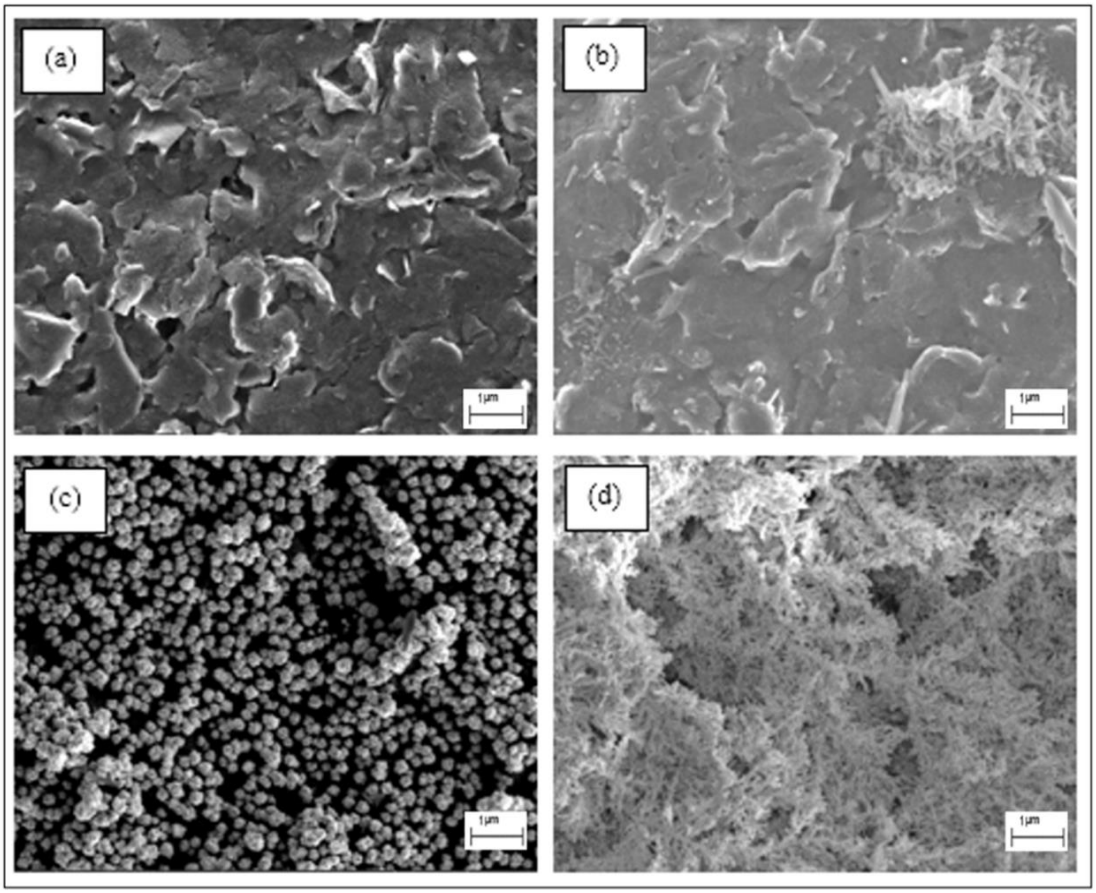

Figure 3. FESEM images at 5000x magnification of (a) bare SPCE and nanogold structures on modified SPCE prepared from 10 mM $HAuCl_4$ + 1.0 M H_2SO_4 at 25 °C for 1800 s at (b) +0.9 V, (c) +0.56 V, and (d) -0.8 V.

Characterisation of Au/SPCE

The applied potential employed for the deposition plays a significant role when it comes to regulating the morphologies and structures of gold. The morphology of nanogold structures was examined using FESEM to determine the effect of electrodeposition potential on the formation of gold structures on the SPCE surface. Figure 3 depicts the surface morphologies of the nanogold structures that were deposited on SPCE for 1800s in a 10 mM $HAuCl_4$ solution under various applied potentials.

Figure 3 shows that irregularly flaking graphite particles covered the unmodified SPCE along its surface. The SPCE deposition at +0.9 V (Figure 3b) consisted of tiny fragments of nanostructure on a certain area of the SPCE surface. There were no significant differences compared with bare SPCE (Figure 3a), while only a certain area of the modified SPCE developed nanostructure fragments. This was due to the low current flow during deposition, which restricted the formation and development of nanostructures. Thus, the gold coating did not completely cover the SPCE surface.

Meanwhile, Figure 3c for +0.56 V potential shows the quasi-spherical nanostructures shaped like gold's morphology that dispersed completely on the SPCE surface with particle sizes less than 5 μm. The electrodeposition at -0.8 V resulted in some dense and rough nanogold structures on the SPCE that had large micrometres of stems and feather-like branches, as seen in Figure 3d.

The elemental composition of nanogold structures on modified SPCE prepared at different deposition potentials is shown in Table 1, as analysed by EDX. The analysis showed no Au present at +0.9 V in the coated SPCE. Due to the extremely low current flow during the deposition process, the amount of Au was almost insignificant, as proven by the FESEM image in Fig. 3b. Meanwhile, at +0.56 V, 98.86 wt. % of gold were detected, and a low amount of oxide formed, indicating that the nanogold structure had been completely deposited on the SPCE surface. However, at -0.8 V potential, HER was taking effect, causing the amount of Au to decrease to 63.62 wt. %. This is a result of H_2 bubbles at the SPCE surface forming and preventing gold from depositing on the entire surface of SPCE [10].

XRD analysis was performed to determine the monocrystalline nature and crystallite sizes of the produced nanogold structures. Bare SPCE was included for comparison with other modified SPCE. According to Zaki et al. (2020) and Sujitha & Kannan (2013), the characteristic facets of gold nanoparticles had proven to appear at (111), (200), (220), and (311) planes using XRD analysis [10][15]. Based on the diffractograms as shown in Figure 4, deposition at +0.56 V exhibited four diffraction peaks of nanogold structures (JCPDS 002-1096) at 2θ and planes with 38.4° (111), 44.7° (200), 65.0° (220), and 78.1° (311). Besides, similar Au diffraction peaks for the gold coating (JCPDS 002-1097) deposited at -0.8 V were identified at 2θ = 38.4°, 44.6°, 65.0°, and 78.1°, which corresponded to (111), (200), (220), and (311), respectively. The XRD analysis demonstrated that all the Au coatings contained pure crystalline Au. However, the deposition at +0.9 V exhibited identical diffraction peaks with bare SPCE, thus it can be concluded that the Au element was almost insignificant.

Electrochemical Performance of AuNP/SPCE

CV was performed for bare SPCE and all gold electrodes in a 0.5 M H_2SO_4 solution to evaluate the electrochemical properties, including the electrochemical active surface area (ECSA). The cyclic voltammograms of modified SPCE at various deposition potentials in a 0.5 M H_2SO_4 solution are shown in Figure 5.

The development of nanogold on the SPCE surface would enhance the ECSA of the electrode, which would increase the number of active sites present on the electrode. This will improve the electrocatalytic performance of the SPCE. The electrochemical characteristics of the modified electrode, in particular, the active surface area of the modified SPCE electrodes, were significantly influenced by the deposition potential.

Table 1. The elemental composition of nanogold structures on modified SPCE prepared at different deposition potentials.

Deposition Potential (V)	Surface Composition (Weight (wt. %))		
	Au	O	C
+0.9	0.00	37.77	62.23
+0.56	98.86	1.14	0.00
-0.8	63.62	ND	36.38

ND = Not Detected

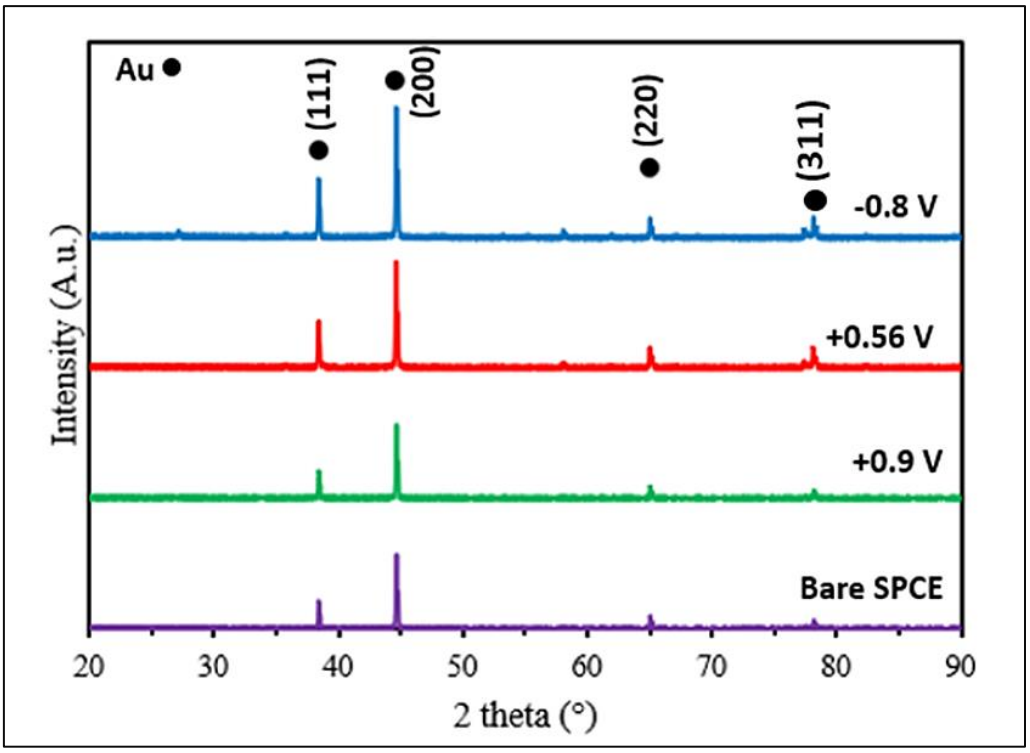

Figure 4. XRD diffractograms of bare SPCE and gold coatings deposited at -0.8 V, +0.56 V, and +0.9 V by chronoamperometry from 10 mM $HAuCl_4$ + 1.0 M H_2SO_4 at 25 °C for 1800s.

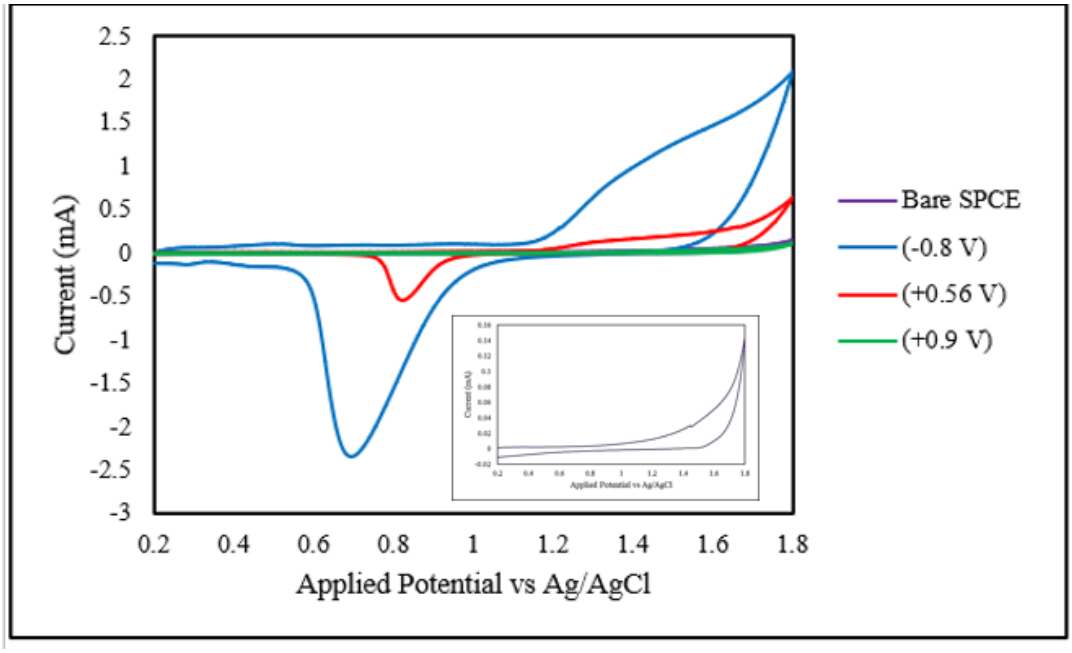

Figure 5. Cyclic voltammograms of electrodeposited gold electrodes with a scan rate of 0.1 V/s in 0.5 M H_2SO_4 solution at different potentials of -0.8 V, + 0.56 V, and + 0.9 V. Inset picture is bare SPCE.

Based on Figure 5, the formation of gold oxide for anodic oxidation of gold started at +1.2 V, while the reduction of gold oxide to gold for cathodic reduction developed in the range of +0.85 V to +0.9 V. However, bare SPCE could only observe the oxidation of water molecules to oxygen, as seen in inset Figure 5, with no reduction current response recorded. Oxygen was assumed to be chemisorbed in a monoatomic layer of gold coating before the evolution of oxygen gas occurred at higher positive

potential scanning with a one-to-one correspondence with the surface metal atoms; thus, the oxidation on the surface occurred [10]. The surface of the electrode was easily oxidised by oxygen in catalytic reactions, involving oxygen-containing molecules.

The estimation of ECSA at different potentials was calculated using Equation 3. The reference charge density used for a monolayer to be reduced per unit of surface area (Q_{Os}) was 0.386 mC.cm^{-2}. Whereas Q_O was the integral area of the cathodic peak (S) in the CV divided by the scan rate (v), which corresponded to the surface oxide reduction process ($Q_o = \frac{S}{v}$).

$$\text{ECSA} = \frac{Q_o}{Q_{os}} \quad (3)$$

The surface of a solid electrode was generally rough, and the real area of the electrode differed depending on the electrode and might also surpass the geometric area. Equation 4 calculates the roughness factor (R_f) by dividing the ECSA by the geometrical area of the SPCE. Since the unmodified SPCE did not have an integral area of cathodic peak, the working electrode area was from the standard Metrohm DropSens SPCE, which is 0.11 cm^2.

$$R_f = \frac{ECSA}{Geometrical\ area\ of\ SPCE} \quad (4)$$

Table 2 displays the ECSA and R_f values of all nanogold deposited on SPCE at various deposition potentials. There is an increase in the ECSA value when the roughness factor increases. Vafaiee and co-workers (2019) emphasised that when the coating surface becomes rougher, the ECSA value will rise. In this study, the nanogold developed at -0.8 V increased the ECSA and R_f significantly, with values of 6.873 cm^2 and 62.48, respectively. In comparison to other gold coatings placed at various deposition potentials, these values were the greatest. These relate to its morphology, which is previously displayed in Figure 3d.

As illustrated in Figure 6, 10 mM $Fe(CN)_6^{-3/-4}$ was used to dissolve in 0.1 M KCl to determine the electron transfer characteristics of the surface of each SPCE with nanogold. The anodic and cathodic peak current density ratio (Ipa/Ipc) value and potential difference (ΔE) were calculated to determine the reversibility of the unmodified and modified SPCE at different potentials and the electron transferred rate, respectively, as shown in Table 3. The Ipa/Ipc of +0.56 V showed good reversibility as the ratio of the anodic and cathodic peaks was equal to 1. The ΔE was also the lowest, which displayed a good electron transfer rate. The electron transfer should be around 0.059 V as one electron was transferred from the Fe^{2+} ion, as shown in Reaction 5.

$$Fe^{2+} \rightarrow Fe^{3+} + e^- \quad (5)$$

Apparently, bare SPCE showed the lowest anodic and cathodic peak current density ratio (I_{pa}/I_{pc}) value for the Fe $(CN)_6^{3-/4-}$ redox reaction with 0.80 as compared to the modified SPCEs. However, upon modification of the SPCE surface with gold nanostructures, the redox current showed a steep increase. From the redox peaks, the I_{pa}/I_{pc} values obtained were 0.83, 0.89, and 0.97 for gold electrodes prepared at +0.9 V, +0.56 V, and -0.8 V, respectively. After adding nanogold to the SPCE, the elevated values of Ipa/Ipc suggest that these nanogold structures had a large electrochemically active surface area and a quick electron transfer rate [10]. Additionally, the $Fe(CN)_6^{-3/-4}$ redox reduction (at reduction current) on all electrodes was determined to be a quasi-reversible reaction.

Table 2. The electrochemical active surface area (ECSA) and roughness factor (R_f) of gold deposition at different potentials.

Deposited Potential (V)	ECSA (cm^2)	Roughness factor (R_f)
Bare SPCE	0.110	1.000
+0.9	0.235	2.138
+0.56	0.786	7.149
-0.8	6.873	62.48

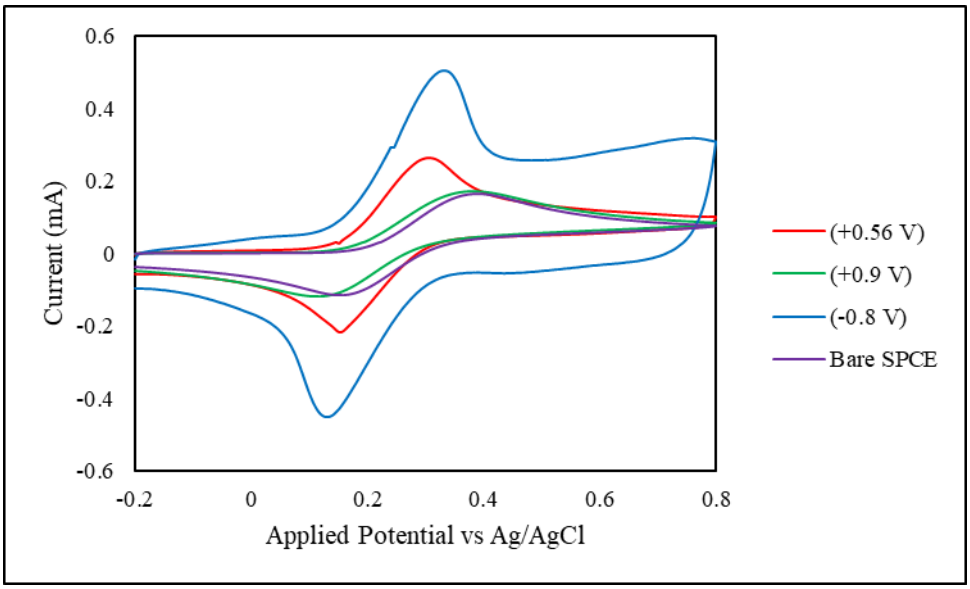

Figure 6. Cyclic voltammograms of bare SPCE and electrodeposited gold electrodes prepared at different potentials of -0.8 V, +0.56 V, and +0.9 V in 10 mM $Fe(CN)_6^{-4}$ + 0.1 M KCl solution at a scan rate of 0.1 V/s.

Table 3. The anodic and cathodic peak current density ratio (Ipa/Ipc) at different potentials.

Deposited Potential (V)	Ipa/Ipc
Bare SPCE	0.80
+0.9	0.83
+0.56	0.89
-0.8	0.97

Henceforth, the effect of $Fe(CN)_6^{-4}$ concentration on the voltametric behaviour of nanogold structures was investigated further, as illustrated in Figure 7. The graph of different concentrations of Fe $(CN)_6^{-4}$ in Figure 8 exhibits excellent linearity with a high correlation coefficient of near to ~1, indicating that the Fe $(CN)_6^{-4}$ oxidation that occurred on the gold coating electrode was a diffusion-controlled process.

Detection of Glucose Using AuNP/SPCE

Since deposition at +0.9 V did not consist of Au as presented in Table 1, two modified electrodes with deposition potentials of +0.56 V and -0.8 V were utilised for further analysis for the detection of glucose because they showed an enhancement in terms of reversibility behaviours in $Fe(CN)_6^{-4}$ solution and also had a large active surface area and roughness factor. Based on Figure 9, the detection of glucose using AuNP/SPCE produced several oxidation peaks in the range of -0.2 V to +0.4 V, which corresponded to the adsorption of the hydroxide (OH^-) ion on the electrode surface, followed by the oxidation of gold-to-gold oxide at around +0.4 V to +0.8 V for the forward scan, and at -0.2 V to +0.2 V in the reverse scan, the gold oxide reduced, and after that, the gold hydroxide layer was desorbed at that potential range [12]. Elmira & Bahram (2020) evaluated the catalytic oxidation of glucose in the negative scan of CV [13].

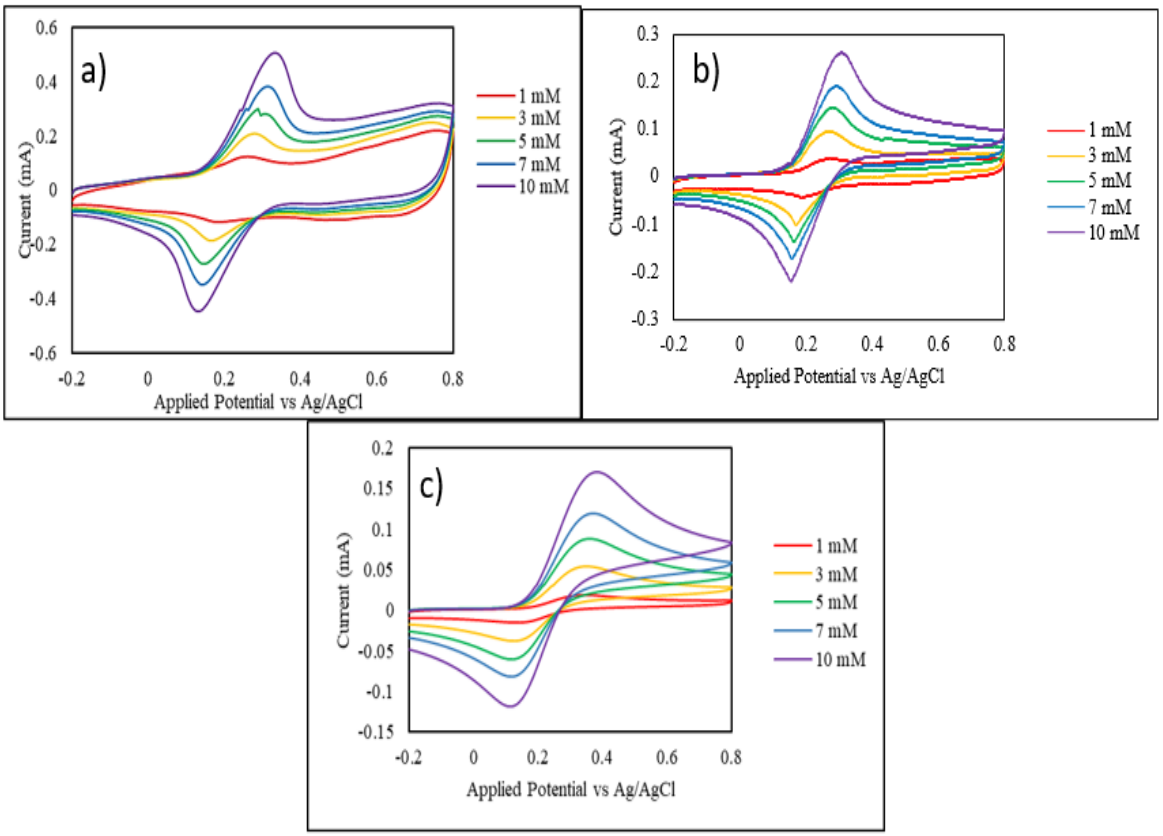

Figure 7. Cyclic voltammograms of gold electrodeposited at (a) -0.8 V, (b) +0.56 V, and (c) +0.9 V potentials at different concentrations of $Fe(CN)_6^{-4}$ in 0.1 M KCl solution with a scan rate of 0.1 V/s.

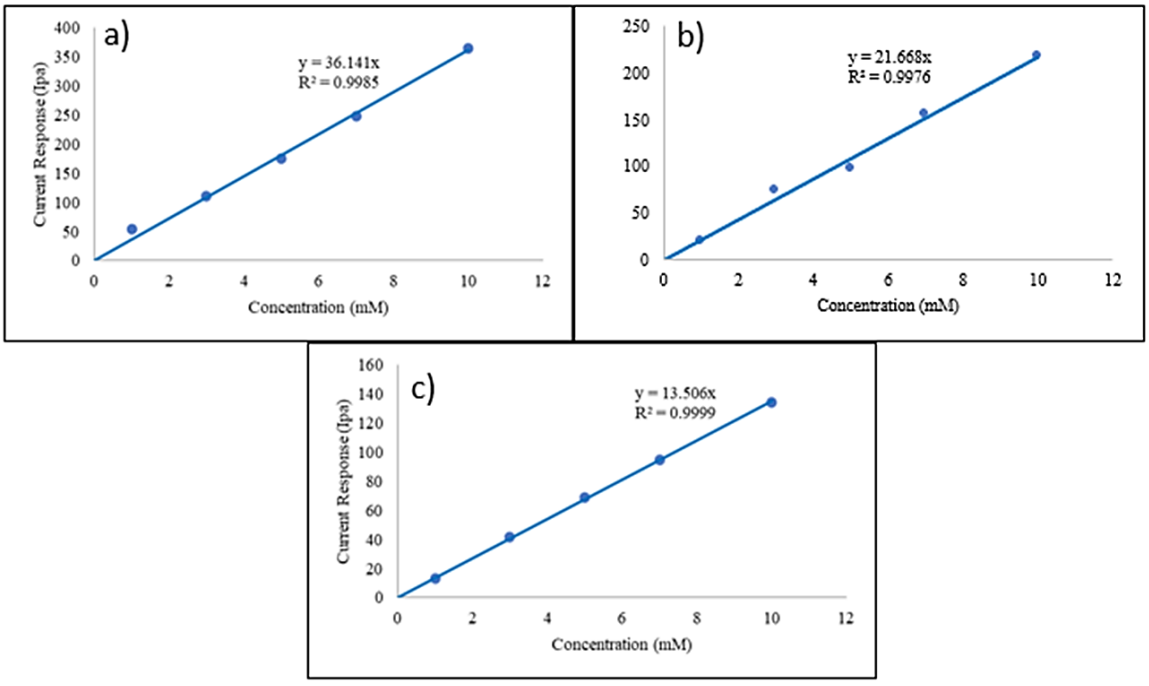

Figure 8. Calibration curves of gold electrodeposited at (a) -0.8 V, (b) +0.56 V, and (c) +0.9 V potentials at different concentrations of $Fe(CN)_6^{-4}$ in 0.1 M KCl solution with a scan rate of 0.1 V/s.

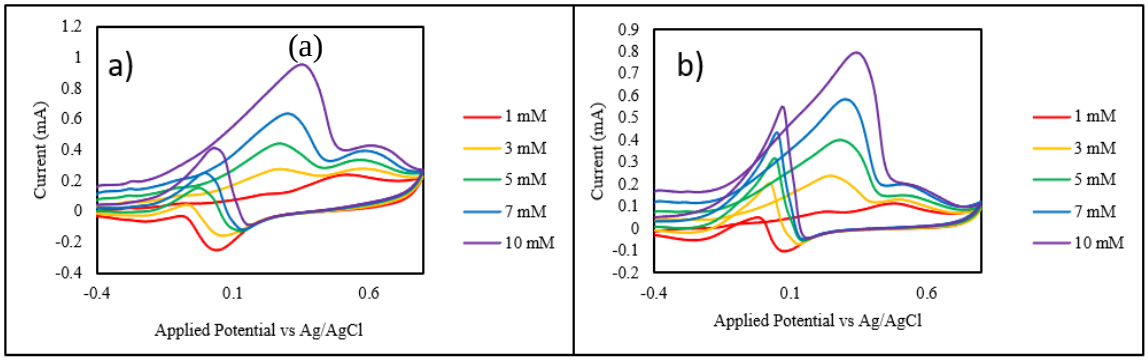

Figure 9. Cyclic voltammograms of AuNP/SPCE deposited at (a) -0.8 V and (b) +0.56 V in different concentrations of glucose in a 0.1 M NaOH solution with a scan rate of 0.1 V/s.

Table 4. The correlation coefficient (R^2), sensitivity, and LOD of AuNP/SPCE deposited at -0.8 V and +0.56 V for the detection of glucose.

Deposited Potential (V)	R^2	Sensitivity (mA.mM^{-1} cm^{-2})	LOD (mM)
-0.8	0.9166	7.53	14.73
+0.56	0.9793	73.38	13.13

However, the oxidation peak in the range of -0.1 V to +0.5 V in the forward scan was chosen for the detection of glucose, and the sensitivity and limit of detection (LOD) are shown in Table 4. Figure 9 shows cyclic voltammograms of AuNP/SPCE deposited at (a) -0.8 V and (b) +0.56 V in different concentrations of glucose in a 0.1 M NaOH solution with a scan rate of 0.1 V/s.

The obtained data showed that the AuNP/SPCE deposited at +0.56 V had higher sensitivity (73.38 mA.mM^{-1} cm^{-2}), a lower detection limit (13.13 mM), and a better linear relationship (R^2 = 0.9793) than deposition at -0.8 V for glucose detection, as presented in Table 4. Therefore, the optimum potential for detection of glucose oxidation on AuNP/SPCE was +0.56 V.

CONCLUSION

The synthesis of AuNP on the surface of SPCE was successfully carried out using the electrodeposition method. The deposition of nanogold structures was analysed using cyclic voltammetry (CV) and chronoamperometry (CA). The deposition potential had affected the morphology and elemental composition of nanogold structures formed on the SPCE surface. The synthesised AuNP was characterised using Field Emission Scanning Electron Microscopy (FESEM) and X-ray Diffraction (XRD). The electrochemical active surface area (ECSA) and roughness factor (R_f) of the nanostructured gold coating deposited at -0.8 V were the highest, with values of 6.873 cm^2 and 62.48, respectively. Meanwhile, ECSA and R_f values with deposition potential of +0.56 V and +0.9 V were 0.786 cm^2 and 7.149, and 0.235 cm^2 and 2.138, respectively. Although the ECSA value for deposited at +0.56 V was not the greatest, the anodic and cathodic peak current density ratios (Ipa/Ipc) showed a great value for reversibility and electron transfer rate. Two modified electrodes, which were deposited at -0.8 V and +0.56 V, respectively, were utilised for the detection of glucose, and both electrodes produced several oxidation peaks on the cyclic voltammograms. The sensitivity and LOD towards glucose were 7.53 mA.mM^{-1} cm^{-2} and 14.73 mM for -0.8 V; 73.38 mA.mM^{-1} cm^{-2} and 13.13 mM for +0.56 V. AuNP/SPCE deposited at +0.56 V gave higher sensitivity and a lower LOD for glucose detection than deposition at -0.8 V.

ACKNOWLEDGEMENTS

This work was financially supported by the Ministry of Education (Malaysia) through the Fundamental Grant Scheme (FRGS) 600-RMI/FRGS 5/3 (094/2019). The authors would like to thank the Faculty of Applied Sciences, Universiti Teknologi MARA (UiTM) Shah Alam, Selangor, for the facilities provided.

REFERENCES

1. World Health Organization (WHO) (2023) *Diabetes, World Health Organization*. https://www.who.int/news-room/fact-sheets/detail/diabetes.

2. Maity, D., Minitha, C. R. and Rajendra Kumar, R.T. (2019) Glucose oxidase immobilized amine

terminated multiwall carbon nanotubes/reduced graphene oxide/polyaniline/gold nanoparticles modified screen-printed carbon electrode for highly sensitive amperometric glucose detection. *Materials Science and Engineering: C*, **105**, 110075. https://doi.org/10.1016/j.msec.2019.110075

3. Govindhan, M., Manickam, S. and Vellaichamy, G. (2018) Electrochemical sensor and biosensor platforms based on advanced nanomaterials for biological and biomedical applications. *Biosensors and Bioelectronics*, **103**, 113–129. https://doi.org/10.1016/j.bios.2017.12.031

4. González-Sánchez, M. I., Gómez-Monedero, B., Agrisuelas, J., Iniesta, J. & Valero, E. (2019) Electrochemical performance of activated screen-printed carbon electrodes for hydrogen peroxide and phenol derivatives sensing. *Journal of Electroanalytical Chemistry*, **839**, 75–82. https://doi.org/10.1016/j.jelechem.2019.03.026

5. Sondhi, P. and Stine, K. J. (2021) Electrodeposition of nanoporous gold thin films. In nanofibers - synthesis, properties and applications. *IntechOpen.* https://doi.org/10.5772/intechopen.94604

6. Francis, N. J. and Knospe, C. R. (2019) Fabrication and characterization of nanoporous gold electrodes for sensor applications. *Advanced Engineering Materials*, **21(3)**, 1800857. https://doi.org/10.1002/adem.201800857

7. Liu, J., Yuan, X., Gao, Q., Qi, H. and Zhang, C. (2012) Ultrasensitive DNA detection based on coulometric measurement of enzymatic silver deposition on gold nanoparticle-modified screen-printed carbon electrode. *Sensors and Actuators B: Chemical*, **162(1)**, 384–390. https://doi.org/10.1016/ j.snb.2011.12.109

8. Cui, M., Huang, T., Xu, J. and Xiao, R. (2022) Homogeneously bimodal nanoporous copper by laser processing-dealloying approach. *Journal of Manufacturing Processes*, **73**, 815–821. https://doi.org/10.1016/j.jmapro.2021.11.054

9. McCormick, W., McDonagh, P., Doran, J. and McCrudden, D. (2021) Covalent immobilisation of a nanoporous platinum film onto a gold screen-printed electrode for highly stable and selective non-enzymatic glucose sensing. *Catalysts*, **11(10)**, 1161. https://doi.org/10.3390/catal11101161

10. Zaki, M. H. M., Mohd, Y. and Chin, L. Y. (2020) Surface properties of nanostructured gold coatings electrodeposited at different potentials. *Int. J. Electrochem. Sci.*, **15**, 11401–11415.

11. Zaki, M. H. M., Mohd, Y. and Isa, N. N. C. (2022) Effects of electrolyte pH on the electro-deposition of nickel on zincated aluminium surfaces. *Malaysian Journal of Chemistry*, **24(1)**, 138–147.

12. Shu, H., Cao, L., Chang, G., He, H., Zhang, Y. and He, Y. (2014) Direct electrodeposition of gold nanostructures onto glassy carbon electrodes for non-enzymatic detection of glucose. *Electro chimica Acta*, **132**, 524–532.

13. Elmira, R. and Bahram, H. (2020) Dendrite gold nanostructures electrodeposited on paper fibers: Application to electrochemical non-enzymatic determination of glucose. *Sensors and Actuators B: Chemical*, **304**, 127335. https://doi.org/10.1016/j.snb.2019.127335

14. Gotti, G., Fajerwerg, K., Evrard, D. and Gros, P. (2014) Electrodeposited gold nanoparticles on glassy carbon: Correlation between nanoparticles characteristics and oxygen reduction kinetics in neutral media. *Electrochimica Acta*, **128**, 412–419.

15. Sujitha, M. V. and Kannan, S. (2013) Green synthesis of gold nanoparticles using Citrus fruits (*Citrus limon, Citrus reticulata and Citrus sinensis*) aqueous extract and its characterization. *Spectrochimica Acta Part A: Molecular and Biomolecular Spectroscopy*, **102,** 15–23.